Absence of giant spin splitting in the two-dimensional electron liquid at the surface of $SrTiO_3$ (001)

S. McKeown Walker,[1,*] S. Riccò,[1] F. Y. Bruno,[1] A. de la Torre,[1] A. Tamai,[1] E. Golias,[2] A. Varykhalov,[2] D. Marchenko,[2] M. Hoesch,[3] M. S. Bahramy,[4,5] P. D. C. King,[6] J. Sánchez-Barriga,[2] and F. Baumberger[1,7]

[1]*Department of Quantum Matter Physics, University of Geneva, 24 Quai Ernest-Ansermet, 1211 Geneva 4, Switzerland*

[2]*Helmholtz-Zentrum Berlin für Materialien und Energie, Albert-Einstein-Str. 15, 12489 Berlin, Germany*

[3]*Diamond Light Source, Harwell Campus, Didcot OX11 0DE, United Kingdom*

[4]*Quantum-Phase Electronics Center, Department of Applied Physics, The University of Tokyo, Tokyo 113-8656, Japan*

[5]*RIKEN Center for Emergent Matter Science (CEMS), Wako 351-0198, Japan*

[6]*SUPA, School of Physics and Astronomy, University of St Andrews, St Andrews, Fife KY16 9SS, United Kingdom*

[7]*Swiss Light Source, Paul Scherrer Institut, CH-5232 Villigen PSI, Switzerland*

(Received 19 February 2016; revised manuscript received 25 May 2016; published 22 June 2016)

We reinvestigate the putative giant spin splitting at the surface of $SrTiO_3$ reported by Santander–Syro *et al.* [Nat. Mater. **13**, 1085 (2014)]. Our spin- and angle-resolved photoemission experiments on fractured (001) oriented surfaces supporting a two-dimensional electron liquid with high carrier density show no detectable spin polarization in the photocurrent. We demonstrate that this result excludes a giant spin splitting while it is consistent with the unconventional Rashba-like splitting seen in band structure calculations that reproduce the experimentally observed ladder of quantum confined subbands.

DOI: 10.1103/PhysRevB.93.245143

Two-dimensional electron liquids (2DELs) formed at the interfaces between insulating transition metal oxides are important for the rapidly growing field of oxide electronics. Their potential utility lies in their exotic responses to external fields which, for the prototypical case of the $LaAlO_3/SrTiO_3$ (LAO/STO) interface, includes gate-tunable superconductivity [1,2] possibly coexisting with magnetism [3], and gate-tunable Rashba interaction [4–6]. It has been shown that STO can support such a two-dimensional electron liquid in many other configurations; for example, when interfaced with amorphous LAO [7], by electrolyte gating [8,9], or by reduction of the bare surface by UV radiation [10,11] or Al capping [12]. Irrespective of their origin, all these systems show a similar electronic structure with multiple subbands and a characteristic orbital polarization, commonly understood as a consequence of quantum confinement of the Ti t_{2g} states in a potential well induced by band bending [10,11,13–18].

Ab initio density functional theory (DFT) of both interface and surface geometries predicts an unconventional Rashba-like spin splitting of these quantum confined subbands due to broken inversion symmetry and the interplay of orbital and spin degrees of freedom. The lifting of spin degeneracy is found to be of the order of ∼1 meV at the Fermi surface except in the vicinity of avoided crossings of subbands with different orbital character where it can be enhanced by almost an order of magnitude [16,19–26]. The resulting k-space spin texture is complex and has not yet been observed experimentally. However, the magnitude and carrier-density dependence of the Rashba splitting inferred from transport and quantum oscillation experiments [4,5,9,27] are in good agreement with these calculations.

Recently, a completely different interpretation of the basic electronic structure of the 2DEL at the (001) surface of STO has been proposed by Santander–Syro *et al.* to explain a large spin polarization signal in their spin- and angle-resolved photoemission spectroscopy (SARPES) measurements [28]. The authors of Ref. [28] propose that the first two light subbands of the STO 2DEL (SB1, SB2 in Fig. 1) arise from a single band with a giant Rashba splitting of approximately 100 meV at the chemical potential. In order to reconcile this claim with the large subband splitting at the Γ point that is well established from high-resolution angle-resolved photoemission spectroscopy (HR-ARPES)[10–12,14,16], Santander–Syro *et al.* propose the existence of strong ferromagnetism with significant out-of-plane moments. To date, a Rashba splitting of this magnitude has not been reproduced experimentally or explained theoretically [23,24,29]. Moreover, a giant Rashba splitting is inconsistent with transport measurements of both electrolyte-gated [8,9] and interface [4,5] 2DELs in STO. It is also far greater than experimentally observed spin-splittings in other systems with broken inversion symmetry whose constituent atoms, like STO, have relatively low atomic numbers leading to a weak atomic spin-orbit interaction [30,31].

Here we present low-temperature SARPES measurements on fractured STO that show a negligible spin polarization of the photocurrent. We demonstrate that this result is consistent with band structure calculations that reproduce the experimentally observed ladder of subbands as well as the Rashba splitting deduced from transport experiments, while it is inconsistent with the giant spin splitting reported by Santander–Syro *et al.* [28].

Single crystals of commercially grown (Crystal Base), lightly electron doped $Sr_{1-x}La_xTiO_3$ (001) ($x = 0.001$) were measured. The La doping results in a small residual bulk conductivity which helps to eliminate charging effects during ARPES measurements but does not otherwise influence our results. HR-ARPES measurements were performed at a temperature of 10 K with a Scienta R4000 hemispherical analyzer at the I05 beamline of the Diamond Light Source with angular resolution $<0.3^\circ$, energy resolution <15 meV, and pressures $<1 \times 10^{-10}$ mbar. SARPES experiments were performed at a temperature of 20 K at pressures $<1 \times 10^{-10}$ mbar, using polarized undulator radiation at the UE112-PGM1 beamline

*siobhan.mckeown@unige.ch

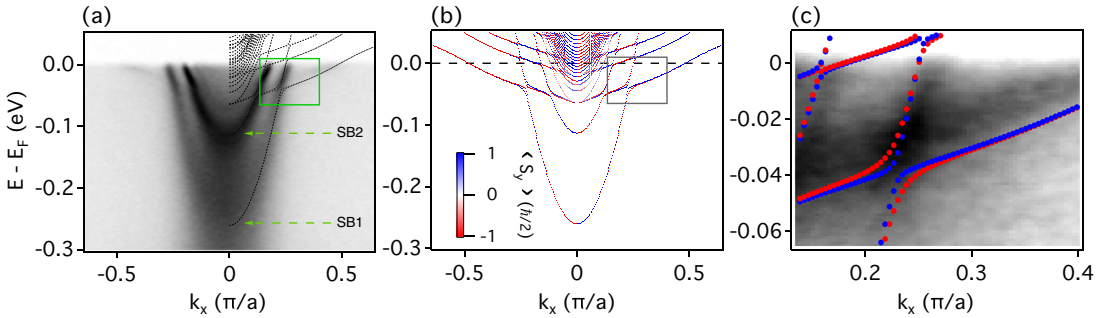

FIG. 1. (a) Subband structure of the STO (001) surface 2DEL from HR-ARPES (grayscale plot) taken at 47 eV with s-polarized light along the [100] direction. Note that throughout this paper all momenta are given relative to the Γ point of the second Brillouin zone at $(k_x,k_y) = (2\pi/a,0)$. The result of self-consistent tight-binding supercell calculations is over-plotted (black dashed lines). (b) Band structure calculation from panel (a) with color-coded spin expectation values $\langle S_y \rangle$. (c) Region of energy-momentum space indicated by the green box in panel (a), measured with p-polarized light at 47 eV to enhance the intensity of the heavy subband which has out-of-plane orbital character.

of BESSY II. Spin analysis of the photoelectrons was provided by a Rice University Mott-type spin polarimeter [32] operated at 26 kV and coupled to a SPECS Phoibos 150 hemispherical analyzer. The energy resolution of the SARPES experiment was ∼100 meV, the angular resolution ∼0.8°, and the Sherman function $S_{\text{eff}} = 0.16$. Samples were fractured *in situ* at the measurement temperature and pressure.

We first demonstrate that our HR-ARPES data are consistent with a subband structure resulting from quantum confinement of the STO conduction band and the ensuing unconventional Rashba spin splitting predicted by several authors [16,19–26,33]. Figure 1(a) shows the energy-momentum dispersion of the (001) STO surface 2DEL measured with spin-integrated HR-ARPES. Three bands with a light band mass and a fourth with a comparatively heavy band mass can be identified. The light bands have d_{xy} orbital character and are more spatially confined than the heavy band of $d_{xz/yz}$ orbital character [16]. The ordering and confinement energies of these subbands are in good agreement with the band structure calculation following the approach of Refs. [16,34], which is overlaid on the right-hand side of Fig. 1(a). This calculation is the self-consistent solution of the coupled Poisson–Schrödinger equations with a tight-binding supercell Hamiltonian obtained from transfer integrals generated by downfolding *ab initio* DFT wave functions onto maximally localized Wannier functions. A band-bending potential has been included as an on-site potential term. The electrostatic boundary conditions are chosen to conserve bulk charge neutrality and reproduce the total experimental bandwidth of ≈250 meV. We include an electric-field-dependent dielectric constant of the form suggested in Ref. [35]. Further details of the calculation can be found elsewhere [16,34].

A small Rashba-like spin splitting is apparent throughout the calculated subband structure. The spin expectation value $\langle S_y \rangle$ of each eigenstate is represented by the red-white-blue color scale in Fig. 1(b) and corresponds to spins locked perpendicular to the momentum. This is the characteristic signature of the Rashba interaction resulting from broken inversion symmetry, which in this case arises from the band bending potential at the surface. However, it is evident from Fig. 1(c) that the spin splitting deviates from a conventional Rashba picture near avoided crossings of light and heavy bands, as found previously in Refs. [16,19–26,33]. In these limited regions of k-space the wave functions are linear combinations of the t_{2g} crystal-field eigenstates. Hence, their orbital angular momentum $\mathbf{L}$ is no longer fully quenched, leading to a sizable spin-orbit coupling $\mathbf{L}\cdot\mathbf{S}$ and thus an enhanced spin splitting [16]. A more detailed comparison with the data shown in Fig. 1(c) highlights that the predicted spin splitting, even at the avoided crossings where it can be as large at 7 meV, would be obscured by resolution and lifetime broadening in HR-ARPES and, as such, is consistent with the experimentally determined subband structure.

While the agreement between our band structure calculations and spin-integrated HR-ARPES data is hard to reconcile with a giant Rashba splitting as reported by Ref. [28], it does not fully exclude it. Therefore, to reinvestigate this discrepancy, we performed new SARPES measurements on fractured surfaces of (001) orientated La doped STO, as were used for the measurements in Fig. 1. To characterize the sample surface prior to the spin-resolved measurements, we acquired the spin-integrated dispersion shown in Fig. 2(b), which confirms the presence of a 2DEL. The lower data quality as compared to Fig. 1 can be attributed to resolution effects. To demonstrate this we show in Fig. 2(c) a two-dimensional convolution of the HR-ARPES measurement in Fig. 1(a) with a Gaussian, representing the energy and momentum resolution of our SARPES measurements. Comparison of Figs. 2(b) and 2(c) confirms that the states have similar carrier density. The slight difference in spectral weight distribution between Figs. 2(b) and 2(c) can be attributed to the different experimental geometry and photon energy of these measurements.

Our SARPES measurements are sensitive to the two components of the spin polarization vector in the Mott scattering plane. In the sample reference frame these correspond to the y component of the spin polarization vector that lies entirely in the surface plane and is perpendicular to the electron momentum k_x, and a combination of the x component and out-of-plane z component. The corresponding spin-resolved energy distribution curves (EDCs) are denoted by $I_i^{\uparrow}$ and $I_i^{\downarrow}$, where $i = y$ or $i = x/z$, respectively. These are calculated from the left and right channeltron count rates I_i^{L} and I_i^{R} by

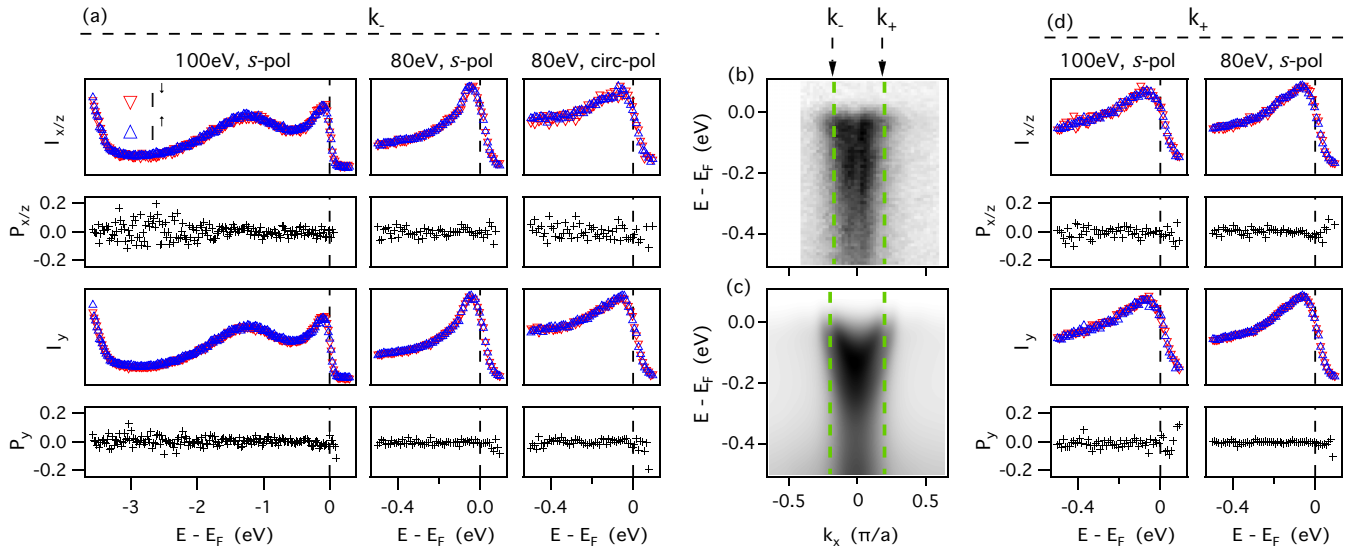

FIG. 2. (a) Spin-resolved photoemission from the STO (001) surface 2DEL at k_- defined in panel (b). Photon energy and polarization are indicated for each column. First row panels show spin-up (blue symbols) and spin-down (red symbols) energy distribution curves for the x/z component of the spin polarization vector calculated from Eq. (1). Second row panel show the corresponding polarization calculated from Eq. (2) with $S_{\rm eff} = 0.16$. Third and fourth row panels are analogous to the first and second rows but for the y component of the spin polarization vector. (b) Spin-integrated dispersion taken with 80 eV s-polarized photons. (c) High-resolution spin-integrated dispersion from Fig. 1(a) convolved with a 2D Gaussian of width of 0.06 Å^{-1} and 90 meV to simulate the experimental resolution. (d) Same as panel (a) at the momentum k_+ as defined in panel (b). The experimental geometry of SARPES measurements was the same as in Ref. [28].

using the standard expressions

$$I_i^{\uparrow} = \tfrac{1}{2}\big(I_i^L + I_i^R\big)(1 + P_i),$$
$$I_i^{\downarrow} = \tfrac{1}{2}\big(I_i^L + I_i^R\big)(1 - P_i), \tag{1}$$

where P_i is the spin polarization given by

$$P_i = \frac{1}{S_{\rm eff}} \frac{I_i^L - I_i^R}{I_i^L + I_i^R} = \frac{I_i^{\uparrow} - I_i^{\downarrow}}{I_i^{\uparrow} + I_i^{\downarrow}}, \tag{2}$$

and $S_{\rm eff} = 0.16$ is the effective Sherman function. Prior to the calculation of $I_i^{\uparrow}$ and $I_i^{\downarrow}$ we subtracted a constant background from the EDCs $I_i^{\rm L}$ and $I_i^{\rm R}$ to account for detector dark counts and the photocurrent due to higher harmonics of the exciting radiation. Subsequently, each EDC pair has been normalized in an energy window where no spin polarization is expected (such as the valence-band maximum) to account for different detector sensitivities.

In Figs. 2(a) and 2(d), the spin-resolved spectra $I_i^{\uparrow}$ (blue symbols) and $I_i^{\downarrow}$ (red symbols) at the momenta $k_{\pm}$ indicated in Fig. 2(b) are shown together with their corresponding polarization signal P_i (black symbols). It is evident from these data that all components of the spin-polarization measured at different photon energies and polarizations are below the noise level. In particular, we do not see any signatures of a Rashba-like spin splitting, which would be expected in the y channel within $\approx$0.3 eV of the Fermi level for the STO surface 2DEL. The upper limit on polarization features that may be obscured by noise in our measurements is $\sim$0.05, which is far smaller than the spin-polarization reported in Ref. [28]. As we will show in the following, our measurements rule out a giant Rashba splitting in our samples, while they are consistent with the much smaller, unconventional Rashba splitting found consistently in our band structure calculations and by several other authors [16,19–26,33].

To facilitate the discussion of our SARPES results, in Fig. 3 we show a minimal simulation of the spin-polarization of the photocurrent expected from the fully-spin-polarized initial states of our band structure calculations shown in Fig. 1. To this end we adopt a noninteracting single-particle description of the photoemission process and neglect all matrix-element effects. In this simple model, $I_y^{\uparrow}$ and $I_y^{\downarrow}$ are found by weighting the poles of the spectral function by the probability $\frac{1}{2} \pm \frac{1}{\hbar}\langle S_y \rangle$. Experimental conditions are taken into account by multiplying $I_y^{\uparrow}$ and $I_y^{\downarrow}$ by the Fermi function at the measurement temperature and convolving the spectral function with a 2D Gaussian of width 120 meV and 0.08 Å^{-1} (corresponding to 0.8°). EDCs for this simulated $I_y^{\uparrow}$ and $I_y^{\downarrow}$ are shown in Figs. 3(a) and 3(c) (blue and red lines, respectively) for the same $k_{\pm}$ as were measured experimentally. The effect of the experimental resolution is evident in the presence of a single broad peak instead of multiple sharp peaks at the energy-momentum positions of the eigenvalues of the calculation in Fig. 1. This broad peak nevertheless shows a small asymmetry which changes sign with k. The P_y corresponding to these EDCs is found by using Eq. (2) and is plotted in Figs. 3(a) and 3(c) as solid gray lines. The features of this simulated polarization signal are $<$0.02, which is below the noise level in our data (black cross symbols). Hence, our experimental resolution, which is similar to that of Ref. [28], completely masks the spin polarization of the initial state. The absence of a significant polarization signal in our SARPES data is thus consistent with the spin-polarized subband structure shown in Fig. 1.

We further note that the simulated polarization signal, shown in Fig. 3(b) over the full range of the 2DEL dispersion,

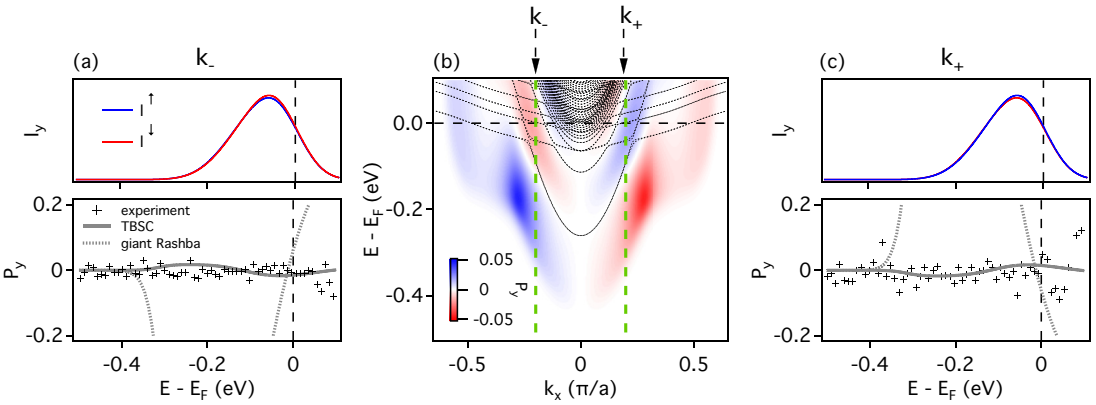

FIG. 3. (a) Upper panel shows the simulated spin-resolved photocurrent intensity $I_y^{\uparrow}$ and $I_y^{\downarrow}$ (blue and red solid lines, respectively) at the momentum k_- defined in panel (b) for the subband structure resulting from tight-binding supercell (TBSC) calculations. Lower panel shows the polarization signal P_y corresponding to $I_y^{\uparrow}$ and $I_y^{\downarrow}$ above (solid gray lines). The simulated P_y signal for a single parabolic band dominated by a 100 meV Rashba spin splitting and Zeeman-like degeneracy lifting at $k_x = 0$ (dashed gray lines). Data from Fig. 2 are over-plotted (black cross symbols). (b) The full energy and momentum dispersion of the simulated spin polarization signal P_y for the TBSC subband structure (black dashed lines) is represented by the red-white-blue color scale. (c) As for panel (a), but for the momentum k_+ defined in panel (b).

has little similarity with the corresponding initial-state polarization shown in Fig. 1(b). SARPES data from complex systems such as the STO 2DEL are thus highly prone to misinterpretation. Indeed, it is nearly impossible to deconvolve the simulation and unambiguously deduce the initial-state polarization from the P_y signal shown in Fig. 3(b). Even with much-improved resolution and detailed knowledge of the subband structure, it would remain challenging to extract the spin texture following the usual fitting procedures. Moreover, in cases like the STO 2DEL, where the predicted spin-splitting is smaller than the intrinsic quasiparticle lifetime broadening over most of energy-momentum space, spin-interference effects will further complicate the interpretation of SARPES data [36]. In this case the initial-state spin polarization can no longer be understood from band structure calculations that neglect interactions and the entire notion of well-defined spin states becomes questionable.

Next, we use the same approach as above to simulate P_y for the single-band electronic structure with a giant Rashba splitting of 100 meV and a Zeeman gap at the Γ point as proposed by Santander–Syro *et al.* [28]. This results in a polarization up to $P_y = \pm 0.9$, shown as gray dashed lines in Figs. 3(a) and 3(c), which is significantly greater than the noise level in our measurements. We can thus unambiguously exclude a Rashba splitting of this magnitude in our data.

In conclusion, we have presented SARPES data from the STO (001) surface 2DEL prepared on *in situ* fractured surfaces with a band dispersion in agreement with all published HR-ARPES data on the surfaces of both fractured STO and *in situ* annealed wafers of STO [10–12,14,16,28,37,38]. Our SARPES measurements do not show any significant spin-polarization signal, which is consistent with the predicted small, unconventional Rashba splitting of the 2DEL subbands. These results exclude the possibility of a giant spin splitting in fractured STO, in contrast with what was reported for *in situ* annealed TiO_2-terminated wafers in Ref. [28]. The origin of this discrepancy remains unclear. It could be related to differences in the surfaces measured in each case. Fractured STO likely has a mixed SrO/TiO_2 termination and, in our experiments, shows a higher surface oxygen vacancy formation rate under UV irradiation than nominally-TiO_2-terminated annealed wafers. This could be relevant since oxygen vacancies have been associated with possible magnetic order in STO 2DELs [23,24,29,39,40]. For example, studying different periodic vacancy arrangements, Altmeyer *et al.* [23] proposed that an SARPES signal as was observed in Ref. [28] might arise from averaging over ferromagnetic domains with exchange-split bands and a remnant Rashba-like spin texture. However, the small in-plane spin component calculated for this scenario is difficult to rationalize with the large spin polarization signal found in Ref. [28]. Moreover, as also noted by Ref. [28], the STO 2DEL subband structure observed by conventional ARPES is ubiquitous and observed consistently for very different surface preparations including those used by Ref. 28 and in the present work [10–12,14,16,37,38]. While we cannot exclude that such a universal band structure could arise from the fundamentally different electronic states proposed here and by Ref. [28], this seems an unlikely coincidence.

This work was supported by the Swiss National Science Foundation (Grant No. 200021-146995). We acknowledge Diamond Light Source for time on beamline I05 under Proposal No. SI11741. Financial support from the Impuls-und Vernetzungsfonds der Helmholtz–Gemeinschaft (Grant No. HRJRG-408) is gratefully acknowledged. P.D.C.K. acknowledges support from the Royal Society through a University Research Fellowship.

[1] N. Reyren, S. Thiel, A. D. Caviglia, L. F. Kourkoutis, G. Hammerl, C. Richter, C. W. Schneider, T. Kopp, A.-S. Rüetschi, D. Jaccard, M. Gabay, D. A. Muller, J.-M. Triscone, and J. Mannhart, Science **317**, 1196 (2007).

[2] A. D. Caviglia, S. Gariglio, N. Reyren, D. Jaccard, T. Schneider, M. Gabay, S. Thiel, G. Hammerl, J. Mannhart, and J.-M. Triscone, Nature (London) **456**, 624 (2008).

[3] L. Li, C. Richter, J. Mannhart, and R. C. Ashoori, Nat. Phys. **7**, 762 (2011).

[4] A. D. Caviglia, M. Gabay, S. Gariglio, N. Reyren, C. Cancellieri, and J.-M. Triscone, Phys. Rev. Lett. **104**, 126803 (2010).

[5] A. Fête, S. Gariglio, C. Berthod, D. Li, D. Stornaiuolo, M. Gabay, and J.-M. Triscone, New J. Phys. **16**, 112002 (2014).

[6] S. Hurand, A. Jouan, C. Feuillet-Palma, G. Singh, J. Biscaras, E. Lesne, N. Reyren, A. Barthélémy, M. Bibes, J. E. Villegas, C. Ulysse, X. Lafosse, M. Pannetier-Lecoeur, S. Caprara, M. Grilli, J. Lesueur, and N. Bergeal, Sci. Rep. **5**, 12751 (2015).

[7] Z. Q. Liu, C. J. Li, W. M. Lü, X. H. Huang, Z. Huang, S. W. Zeng, X. P. Qiu, L. S. Huang, A. Annadi, J. S. Chen, J. M. D. Coey, T. Venkatesan, and Ariando, Phys. Rev. X **3**, 021010 (2013).

[8] K. Ueno, S. Nakamura, H. Shimotani, A. Ohtomo, N. Kimura, T. Nojima, H. Aoki, Y. Iwasa, and M. Kawasaki, Nat. Mater. **7**, 855 (2008).

[9] H. Nakamura, T. Koga, and T. Kimura, Phys. Rev. Lett. **108**, 206601 (2012).

[10] W. Meevasana, P. D. C. King, R. H. He, S.-K. Mo, M. Hashimoto, A. Tamai, P. Songsiriritthigul, F. Baumberger, and Z.-X. Shen, Nat. Mater. **10**, 114 (2011).

[11] S. McKeown Walker, F. Y. Bruno, Z. Wang, A. de la Torre, S. Riccó, A. Tamai, T. K. Kim, M. Hoesch, M. Shi, M. S. Bahramy, P. D. C. King, and F. Baumberger, Adv. Mater. **27**, 3894 (2015).

[12] T. C. Rödel, F. Fortuna, S. Sengupta, E. Frantzeskakis, P. L. Fèvre, F. Bertran, B. Mercey, S. Matzen, G. Agnus, T. Maroutian, P. Lecoeur, and A. F. Santander–Syro, Adv. Mater. **28**, 1976 (2016).

[13] M. Stengel, Phys. Rev. Lett. **106**, 136803 (2011).

[14] A. F. Santander–Syro, O. Copie, T. Kondo, F. Fortuna, S. Pailhès, R. Weht, X. G. Qiu, F. Bertran, A. Nicolaou, A. Taleb-Ibrahimi, P. Le Fèvre, G. Herranz, M. Bibes, N. Reyren, Y. Apertet, P. Lecoeur, A. Barthélémy, and M. J. Rozenberg, Nature (London) **469**, 189 (2011).

[15] A. Joshua, S. Pecker, J. Ruhman, E. Altman, and S. Ilani, Nat. Commun. **3**, 1129 (2012).

[16] P. D. C. King, S. McKeown Walker, A. Tamai, A. de la Torre, T. Eknapakul, P. Buaphet, S.-K. Mo, W. Meevasana, M. S. Bahramy, and F. Baumberger, Nat. Commun. **5**, 3414 (2014).

[17] M. Salluzzo, J. C. Cezar, N. B. Brookes, V. Bisogni, G. M. De Luca, C. Richter, S. Thiel, J. Mannhart, M. Huijben, A. Brinkman, G. Rijnders, and G. Ghiringhelli, Phys. Rev. Lett. **102**, 166804 (2009).

[18] C. Cancellieri, M. L. Reinle-Schmitt, M. Kobayashi, V. N. Strocov, P. R. Willmott, D. Fontaine, P. Ghosez, A. Filippetti, P. Delugas, and V. Fiorentini, Phys. Rev. B **89**, 121412 (2014).

[19] Z. Zhong, A. Tóth, and K. Held, Phys. Rev. B **87**, 161102 (2013).

[20] G. Khalsa, B. Lee, and A. H. MacDonald, Phys. Rev. B **88**, 041302 (2013).

[21] P. Kim, K. T. Kang, G. Go, and J. H. Han, Phys. Rev. B **90**, 205423 (2014).

[22] Y. Kim, R. M. Lutchyn, and C. Nayak, Phys. Rev. B **87**, 245121 (2013).

[23] M. Altmeyer, H. O. Jeschke, O. Hijano-Cubelos, C. Martins, F. Lechermann, K. Koepernik, A. F. Santander–Syro, M. J. Rozenberg, R. Valentí, and M. Gabay, Phys. Rev. Lett. **116**, 157203 (2016).

[24] A. C. Garcia–Castro, M. G. Vergniory, E. Bousquet, and A. H. Romero, Phys. Rev. B **93**, 045405 (2016).

[25] K. V. Shanavas, Phys. Rev. B **93**, 045108 (2016).

[26] L. W. van Heeringen, G. A. de Wijs, A. McCollam, J. C. Maan, and A. Fasolino, Phys. Rev. B **88**, 205140 (2013).

[27] H. Liang, L. Cheng, L. Wei, Z. Luo, G. Yu, C. Zeng, and Z. Zhang, Phys. Rev. B **92**, 075309 (2015).

[28] A. F. Santander–Syro, F. Fortuna, C. Bareille, T. C. Rödel, G. Landolt, N. C. Plumb, J. H. Dil, and M. Radović, Nat. Mater. **13**, 1085 (2014).

[29] S. S. Ghosh and E. Manousakis, arXiv:1511.07495.

[30] A. Tamai, W. Meevasana, P. D. C. King, C. W. Nicholson, A. de la Torre, E. Rozbicki, and F. Baumberger, Phys. Rev. B **87**, 075113 (2013).

[31] D. Marchenko, A. Varykhalov, M. R. Scholz, J. Sánchez-Barriga, O. Rader, A. Rybkina, A. M. Shikin, T. Seyller, and G. Bihlmayer, Phys. Rev. B **88**, 075422 (2013).

[32] G. C. Burnett, T. J. Monroe, and F. N. Dunning, Rev. Sci. Instrum. **65**, 1893 (1994).

[33] J. Zhou, W. Y. Shan, and D. Xiao, Phys. Rev. B **91**, 241302(R) (2015).

[34] M. S. Bahramy, P. D. C. King, A. de la Torre, J. Chang, M. Shi, L. Patthey, G. Balakrishnan, P. Hofmann, R. Arita, N. Nagaosa, and F. Baumberger, Nat. Commun. **3**, 1159 (2012).

[35] O. Copie, V. Garcia, C. Bödefeld, C. Carrétéro, M. Bibes, G. Herranz, E. Jacquet, J.-L. Maurice, B. Vinter, S. Fusil, K. Bouzehouane, H. Jaffrès, and A. Barthélémy, Phys. Rev. Lett. **102**, 216804 (2009).

[36] F. Meier, V. Petrov, H. Mirhosseini, L. Patthey, J. Henk, J. Osterwalder, and J. H. Dil, J. Phys.: Condens. Matter **23**, 072207 (2011).

[37] N. C. Plumb, M. Salluzzo, E. Razzoli, M. Månsson, M. Falub, J. Krempasky, C. E. Matt, J. Chang, M. Schulte, J. Braun, H. Ebert, J. Minár, B. Delley, K.-J. Zhou, T. Schmitt, M. Shi, J. Mesot, L. Patthey, and M. Radović, Phys. Rev. Lett. **113**, 086801 (2014).

[38] Z. Wang, S. McKeown Walker, A. Tamai, Y. Wang, Z. Ristic, F. Y. Bruno, A. de la Torre, S. Riccò, N. C. Plumb, M. Shi, P. Hlawenka, J. Sánchez-Barriga, A. Varykhalov, T. K. Kim, M. Hoesch, P. D. C. King, W. Meevasana, U. Diebold, J. Mesot, B. Moritz, T. P. Devereaux, M. Radovic, and F. Baumberger, Nat. Mater. (2016), doi: 10.1038/nmat4623.

[39] N. Pavlenko, T. Kopp, E. Y. Tsymbal, J. Mannhart, and G. A. Sawatzky, Phys. Rev. B **86**, 064431 (2012).

[40] N. Pavlenko, T. Kopp, E. Y. Tsymbal, G. A. Sawatzky, and J. Mannhart, Phys. Rev. B **85**, 020407 (2012).